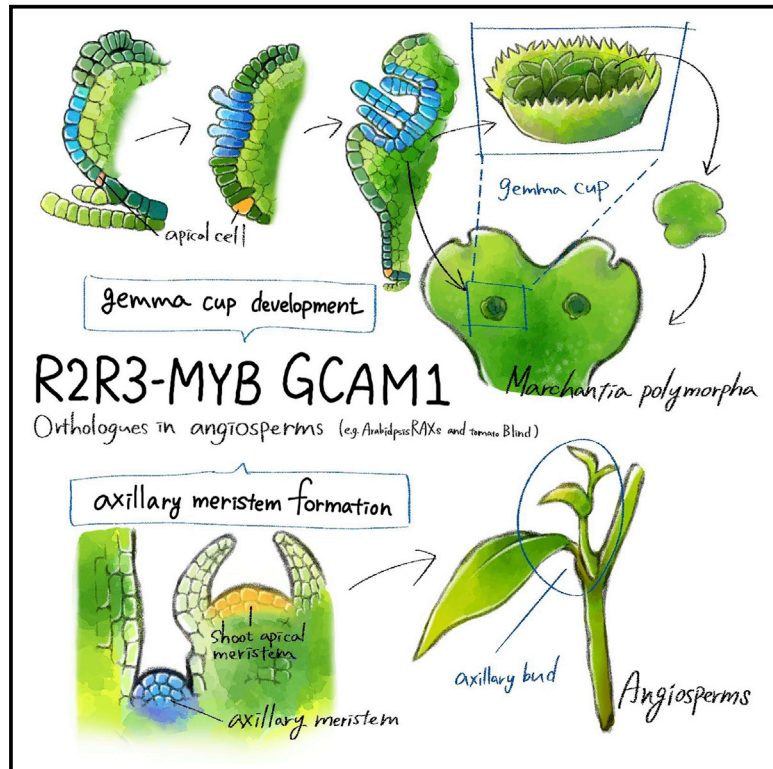


Current Biology

GEMMA CUP-ASSOCIATED MYB1, an Ortholog of Axillary Meristem Regulators, Is Essential in Vegetative Reproduction in *Marchantia polymorpha*

Graphical Abstract



Authors

Yukiko Yasui, Shigeyuki Tsukamoto, Tomomi Sugaya, ..., Klaus Theres, Takayuki Kohchi, Kimitsune Ishizaki

Correspondence

kimi@emerald.kobe-u.ac.jp

In Brief

The gemma cup is a specialized organ that produces clonal progenies, gemmae, in the liverwort *Marchantia polymorpha*. Yasui et al. identify an R2R3-MYB transcription factor, GCAM1, as an essential regulator of gemma cup formation. GCAM1 is an ortholog of regulatory factors of axillary meristem formation in angiosperms.

Highlights

- The gemma cup is a specialized organ that produces clonal progenies in *M. polymorpha*
- An R2R3-MYB, GCAM1, is an essential regulator of gemma cup formation
- Ectopic overexpression of GCAM1 promotes proliferation of undifferentiated cells
- GCAM1 is an ortholog of regulators of axillary meristem formation in angiosperms



GEMMA CUP-ASSOCIATED MYB1, an Ortholog of Axillary Meristem Regulators, Is Essential in Vegetative Reproduction in *Marchantia polymorpha*

Yukiko Yasui,^{1,2,6} Shigeyuki Tsukamoto,^{1,6} Tomomi Sugaya,³ Ryuichi Nishihama,² Quan Wang,⁴ Hirotaka Kato,¹ Katsuyuki T. Yamato,⁵ Hidehiro Fukaki,¹ Tetsuro Mimura,¹ Hiroyoshi Kubo,³ Klaus Theres,⁴ Takayuki Kohchi,² and Kimitsune Ishizaki^{1,7,*}

¹Graduate School of Science, Kobe University, Kobe 657-8501, Japan

²Graduate School of Biostudies, Kyoto University, Kyoto 606-8502, Japan

³Department of Biology, Faculty of Science, Shinshu University, Matsumoto 390-8621, Japan

⁴Department of Plant Breeding and Genetics, Max Planck Institute for Plant Breeding Research, Carl-von-Linné-Weg 10, 50829 Cologne, Germany

⁵Faculty of Biology-Oriented Science and Technology, Kindai University, 930 Nishimitani, Kinokawa, Wakayama 649-6493, Japan

⁶These authors contributed equally

⁷Lead Contact

*Correspondence: kimi@emerald.kobe-u.ac.jp

<https://doi.org/10.1016/j.cub.2019.10.004>

SUMMARY

A variety of plants in diverse taxa can reproduce asexually via vegetative propagation, in which clonal propagules with a new meristem(s) are generated directly from vegetative organs. A basal land plant, *Marchantia polymorpha*, develops clonal propagules, gemmae, on the gametophyte thallus from the basal epidermis of a specialized receptacle, the gemma cup. Here we report an R2R3-MYB transcription factor, designated GEMMA CUP-ASSOCIATED MYB1 (GCAM1), which is an essential regulator of gemma cup development in *M. polymorpha*. Targeted disruption of *GCAM1* conferred a complete loss of gemma cup formation and gemma generation. Ectopic overexpression of *GCAM1* resulted in formation of cell clumps, suggesting a function of GCAM1 in suppression of cell differentiation. Although gemma cups are a characteristic gametophyte organ for vegetative reproduction in a taxonomically restricted group of liverwort species, phylogenetic and interspecific complementation analyses support the orthologous relationship of GCAM1 to regulatory factors of axillary meristem formation, e.g., *Arabidopsis* REGULATOR OF AXILLARY MERISTEMS and tomato Blind, in angiosperm sporophytes. The present findings in *M. polymorpha* suggest an ancient acquisition of a transcriptional regulator for production of asexual propagules in the gametophyte and the use of the regulatory factor for diverse developmental programs, including axillary meristem formation, during land plant evolution.

INTRODUCTION

The plastic nature of plant architecture can be traced back to the activity of meristems, which are pools of pluripotent cells located at the tips of growing plant bodies. In seed plants, the primary shoot apical meristem (SAM) is established during embryonic development. Following germination, secondary meristems are continuously produced in the axils of leaves, and form the basis of branching in flowering plants. Many plant species also develop ectopic meristems at different positions of the plant body [1, 2].

Vegetative reproduction, a form of asexual reproduction in plants, is a developmental process by which clonal progeny arise directly from parental tissues. This process is based on the remarkable potential of plants to proliferate meristems, which develop whole plantlets from differentiated tissues [1, 3, 4]. Diverse plants have the capability for vegetative reproduction, which occurs naturally from a variety of vegetative tissues, e.g., stems (rhizomes: asparagus, iris, ginger; bulbs: onion; tubers: potato; corms: crocus; runners: strawberry, wild mint), roots (sweet potato), and leaves (*Kalanchoe*), or can be induced artificially by means of various techniques, including cuttings, grafting, and tissue culture. Vegetative reproduction is considered to be an important strategy for efficient plant propagation and survival in the natural environment [5], as well as for agriculture and horticulture [6].

The liverwort *Marchantia polymorpha* L., as well as certain related species in the class Marchantiopsida, develops specialized organs for vegetative reproduction, termed the gemma cup or cupule [7]. Clonal propagules, called gemmae, develop from single epidermal cells at the base, or floor, of gemma cups. Thus, the floor cells have the capability to produce clonal plantlets. Gemma cups are formed periodically along the dorsal midrib of a thallus. The restricted occurrence of gemma cups along the midrib suggests that they originate from the dorsal merophyte above the apical cell [7]. Over 100 gemmae can develop in a



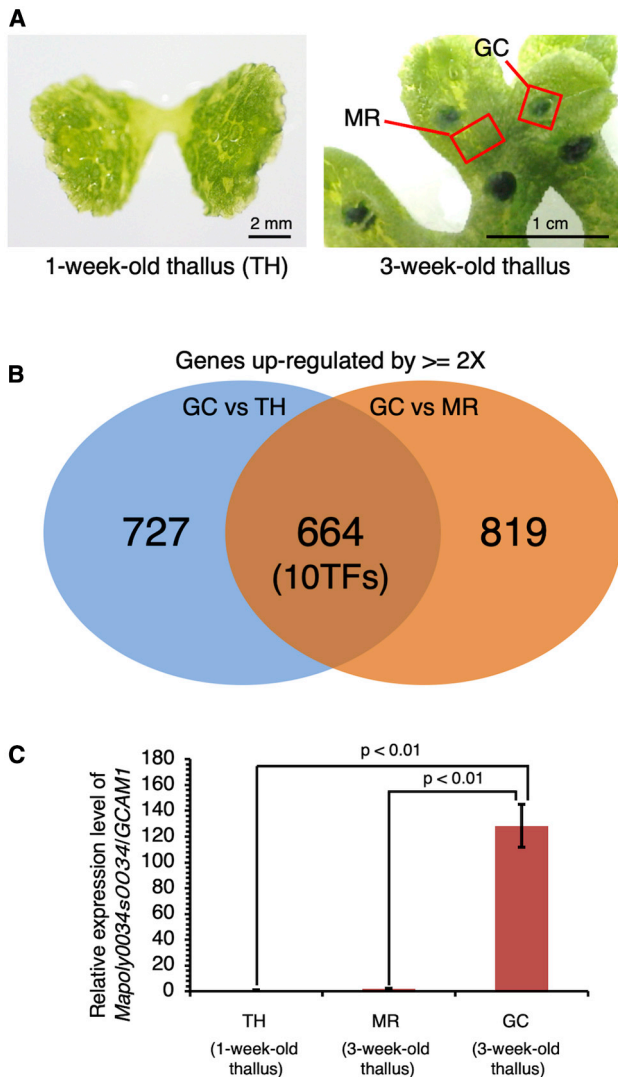


Figure 1. Identification of Genes Preferentially Expressed in the Gemma Cup of *M. polymorpha*

(A) Tissues used for mRNA-seq analysis. GC, gemma cup; TH, 1-week-old thallus; MR, midrib.

(B) Venn diagram of genes upregulated by more than 2-fold in the gemma cup. TF, transcription factor.

(C) qRT-PCR analysis of *Mapoly0034s0034/GCAM1* in vegetative tissues. The elongation factor 1a (*MpEF1a*) gene was used as a reference. Data are displayed as means \pm SD ($n = 3$), and significant differences with Welch's *t* test are indicated ($p < 0.01$).

See [Figure S1](#), [Tables S1](#) and [S2](#), and [Data S1](#) for details.

single gemma cup. The development of gemma cups has been well described on the basis of a series of histological observations of *M. polymorpha* [8]. According to the detailed observations by Barnes and Land [8], the precursors of the floor epidermis in a gemma cup are recognizable as close as the third cell back from the apical cell on the dorsal surface. The floor epidermis is a region where periclinal cell divisions to generate protodermal and subprotodermal cell layers of the air chamber are suppressed, and consecutive elongated epidermal cells are instead observed. The single-layered epidermal cells comprise

the gemminiferous region, an area that will become the basal epidermis of a gemma cup. These cells undergo repeated anticlinal divisions to enlarge the area of the gemma cup floor, allowing for an increase in gemma production. Some gemma cup floor cells begin to develop gemmae from an early stage of gemma cup development, and growth of the gemma cup occurs concomitantly with gemma development and maturation (Figure S1). The frequency of gemma cup formation is influenced by a variety of environmental factors, such as light and nutrients [9–11]. However, the molecular mechanisms underlying gemma and gemma cup development are largely unknown.

M. polymorpha is a member of an early-diverging lineage among land plants. The species offers a number of advantages for genetic studies: low genetic redundancy [12], a haploid-dominant life cycle, and practicable genetic tools, such as high-efficiency transformation and gene modification techniques [13]. Recent molecular genetic studies on bryophytes, including *M. polymorpha*, have revealed several key developmental regulators for gametophyte generation that have orthologous counterparts in angiosperms shown to control analogous, but not homologous, developmental processes in sporophyte generation [14, 15]. These observations suggest that a considerable number of developmental regulatory modules were acquired in the common ancestor of land plants before the divergence of bryophytes and vascular plants.

In the present study, we undertook a comprehensive transcriptome analysis and isolated an R2R3-MYB transcription factor gene, *GEMMA CUP-ASSOCIATED MYB1* (*GCAM1*), which was predominantly upregulated in developing *M. polymorpha* gemma cups. Molecular and genetic characterization revealed a critical role for *GCAM1* in gemma cup development. Cell proliferation without tissue differentiation was observed in plants ectopically expressing *GCAM1*. Although the gemma cup is a characteristic gametophytic organ for vegetative reproduction in certain species of Marchantiopsida, phylogenetic and interspecific complementation analyses supported the orthologous relationship of *GCAM1* with angiosperm genes of R2R3-MYB subfamily 14 [16], which are involved in axillary meristem formation. Potential mechanisms shared between vegetative reproduction in the gametophyte of liverworts and axillary meristem formation in the sporophyte of angiosperms are discussed.

RESULTS

An R2R3-MYB Transcription Factor Is Upregulated in the Gemma Cup

To screen for potential key regulators involved in vegetative reproduction in *M. polymorpha*, we performed RNA sequencing (RNA-seq) analyses comparing the transcriptome of gemma cups with that of the entire young thallus yet to form gemma cups and that of the midrib region (Figure 1A). We obtained more than 14×10^6 reads from each of the samples (triplicates per tissue; Table S1). More than 90% of the reads per library were mapped to *M. polymorpha* genome sequence version 3.1 [12]. Genes for which the reads per kilobase per million (RPKM) value was >1 were considered to be “expressed.” Among the 19,287 annotated genes, 11,699 genes (61%) were expressed in the gemma cup. We identified 1,391 and 1,483 genes with greater than 2-fold changes in the gemma cup

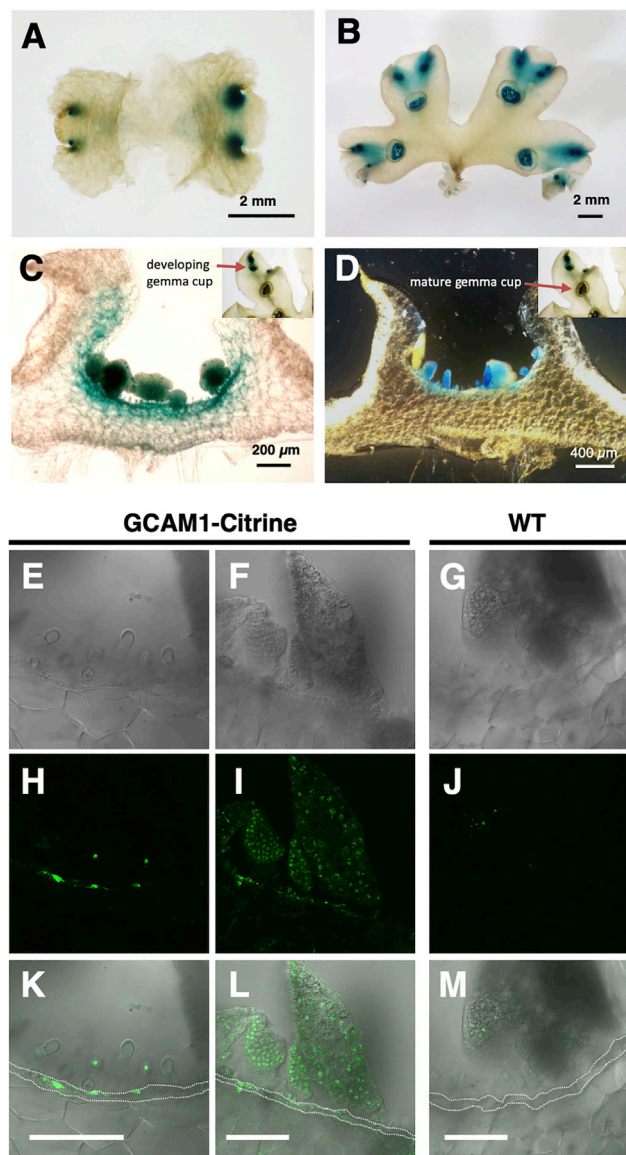


Figure 2. GCAM1 Expression Pattern in the Vegetative Growth Stage of *M. polymorpha*

(A–D) Histochemical GUS assay in a representative *GCAM1pro:GUS* line.

(A) Ten-day-old thallus.

(B) Three-week-old thallus with gemma cups.

(C and D) Transverse sections of developing and mature gemma cups on a 3-week-old thallus. Developing gemma cups are those closely located near the apical notch (C) and mature gemma cups are those located in the basal region of the thallus (D).

(E–M) Accumulation of GCAM1 in the basal floor of the gemma cup. Bright-field (E–G), single-confocal (H–J), and merged (K–M) images of the basal floor of gemma cups in 17- to 18-day-old thalli in *GCAM1-Citrine* knockin plants (E, F, H, I, K, and L) and the WT (G, J, and M). Dotted lines indicate basal floor cells. Scale bars represent 100 μm .

See also Figures S2A–S2C.

compared with their expression in the young thallus and midrib tissue, respectively. A total of 664 genes were upregulated in both comparisons (Figure 1B; Data S1A–S1C). Of the 664 genes, 10 were annotated as transcription factors (Table S2).

Among the transcription factors, we focused on Mapoly0034s0034, a gene encoding an R2R3-MYB transcription factor. The RPKM value of this gene in the gemma cup was 82.1, which represented 100-fold and 13-fold upregulation compared with expression in the young thallus and the midrib, respectively (Table S2). qRT-PCR analysis confirmed that Mapoly0034s0034 transcripts accumulated at a significantly higher level in gemma cups than in the young thallus and midrib tissue (Figure 1C). We designated the *Mapoly0034s0034* gene as *GEMMA CUP-ASSOCIATED MYB1* (*GCAM1*). Genetic nomenclature is as outlined in Bowman et al. [17].

Next, we generated transgenic *M. polymorpha* plants expressing a β -glucuronidase (GUS) reporter gene under the control of the *GCAM1* promoter (*GCAM1pro:GUS*). We generated a construct in which the GUS reporter gene was translationally fused to a *GCAM1* genomic fragment containing 5.2 kb upstream of the ATG start codon. In *GCAM1pro:GUS* transgenic lines, histological GUS staining was detected in the apical notches of 10-day-old thallus (Figure 2A). In mature thalli with gemma cups, significant promoter activity was detected in the apical notches, the floor of gemma cups, and developing gemmae (Figures 2B–2D).

To analyze the localization of protein accumulation, we inserted the yellow fluorescent protein (Citrine) sequence into the 3' end of the *GCAM1* coding sequence (CDS) in the *M. polymorpha* genome (Figures S2A and S2B). The *GCAM1-Citrine* knockin plants exhibited normal organ development, including gemma cups during vegetative growth (Figure S2C). Consistent with the promoter-reporter analysis, we detected Citrine signals in the nucleus of cells in the developing gemma and gemma cup floor cells (Figures 2E–2M).

GCAM1 Is Essential for Gemma Cup Formation

To investigate the function of *GCAM1*, we disrupted *GCAM1* using homologous-recombination-mediated gene targeting technology [18]. Two independent *GCAM1* knockout lines (*gcam1^{ko}*) were isolated from 522 candidates (Figures S2D and S2E). RT-PCR demonstrated that no transcripts spanning the hygromycin-resistant cassette were detected in the *gcam1^{ko}* plants, whereas truncated *GCAM1* transcripts were detected at a low level (Figure S2F). Because the *gcam1^{ko}* plants lack half of the R2R3-MYB DNA-binding domain, we concluded that no functional transcript of *GCAM1* was expressed in *gcam1^{ko}* plants. In the wild type, 3-week-old thallus developed from a thallus explant containing an apical notch, and over ten gemma cups filled with gemmae were observed on the midrib of the dorsal surface (Figures 3A, 3C, and 3E). In contrast, no gemma cup development was observed on the dorsal surface of the *gcam1^{ko}* midrib (Figures 3B and 3D), resulting in no gemma generation. No distinct impairment of thallus growth or development of other vegetative organs, i.e., air chamber, rhizoid, and ventral scales, was observed in *gcam1^{ko}* thalli compared with those of wild-type (WT) thalli (Figures 3C–3F). We also generated *GCAM1* mutants using CRISPR/Cas9-mediated targeted genome editing [19, 20]. Two independent *GCAM1* mutants for each of two independent target sequences of *GCAM1* exhibited absence of gemma cup development, but no other obvious aberrant phenotype was observed during vegetative growth (Figure S3), and thus the phenotypes were essentially identical to those of

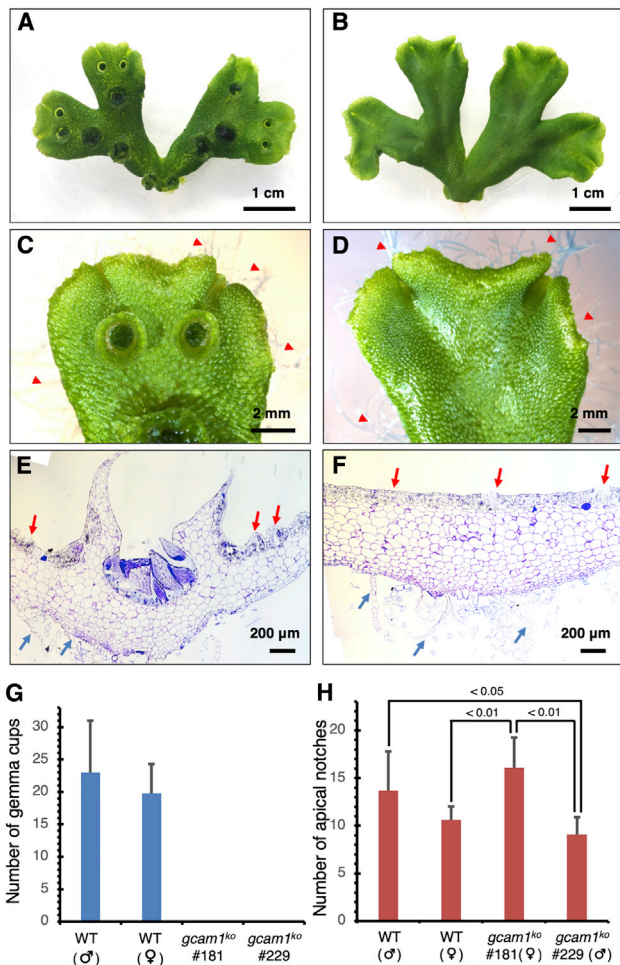


Figure 3. Phenotype of the *gcam1* Mutant of *M. polymorpha*

(A and B) Three-week-old thalli grown from the tip of thalli of the WT (A) and *gcam1^{ko}* knockout mutant (B). The thalli were grown from the tip of parental thalli, because gemmae were absent in *gcam1^{ko}* lines.

(C and D) Close-up of the tip of thalli of the previous individual, showing gemma cups in the WT (C), whereas gemma cups were absent in the *gcam1^{ko}* lines (D). Red arrowheads indicate rhizoids.

(E and F) Transverse sections (5 μ m thick) from 3-week-old thalli of the WT (E) and *gcam1^{ko}* (F). Red and blue arrows indicate air chambers and ventral scales, respectively.

(G) Number of gemma cups in the WT and *gcam1^{ko}* lines.

(H) Number of apical notches in the WT and *gcam1^{ko}* lines.

Values are means \pm SD (n = 10), and significant differences detected with Welch's t test are indicated.

See also Figures S2D–S2F and S3.

gcam1^{ko} plants. Altogether, these results demonstrated that *GCAM1* performs a critical role in gemma cup formation.

Generation of gemma cups is correlated with bifurcation (i.e., branching of the apical meristem) of thalli [7]. To clarify whether *GCAM1* may also be involved in branching, we investigated the number of gemma cups and apical notches in the *gcam1^{ko}* line in comparison with those of the WT. About 20 gemma cups were observed on 3-week-old WT thalli, whereas no gemma cups developed in the *gcam1^{ko}* mutants (Figure 3G). In contrast to the conspicuous gemma cup phenotype, *gcam1^{ko}* lines showed

periodic bifurcations at a similar frequency to that of the WT (Figure 3H). Although there were significant differences in the number of apical notches between Tak-1 and *gcam1^{ko}* 229 (male), and Tak-2 and *gcam1^{ko}* 181 (female), the trends of differences between the WT and *gcam1^{ko}* lines were opposite in the sexual background (Figure 3H), which could be caused by polymorphisms in the F₁ population. These results suggest that *GCAM1* does not play a major role in bifurcation of the thallus apical notch.

Overexpression of *GCAM1* Promotes Proliferation of Undifferentiated Cells

To further investigate the developmental function of *GCAM1*, we generated transgenic plants that ectopically overexpressed *GCAM1* under the control of the Mp*ELONGATION FACTOR 1 α* regulatory sequence in *M. polymorpha* (Mp*EFpro:GCAM1*). We obtained a significantly lower number of transformants using the Mp*EFpro:GCAM1* construct than usual, and the majority of the obtained Mp*EFpro:GCAM1* lines formed a mass of tiny flat thallus-like structures (Figures S4A–S4F). Thus, we utilized an inducible system (Figure 4A), in which protein nuclear localization is modulated by a glucocorticoid receptor (GR) domain [21, 22]. In these transgenic plants, *GCAM1* function was expected to be induced by treatment with dexamethasone (DEX). In the WT, treatment with DEX caused no morphological effect (Figures S4G–S4L). In the absence of DEX, Mp*EFpro:GCAM1-GR* plants exhibited the WT phenotype and formed normal dorsal/ventral organs, i.e., air chambers, gemma cups, scales, and rhizoids (Figures 4B, 4D, and 4F). Treatment of Mp*EFpro:GCAM1-GR* plants with DEX severely suppressed thallus growth, and cell clumps with no dorsal/ventral organs and few rhizoids were observed (Figures 4C, 4E, and 4G). After suspension of the DEX treatment, a number of small thallus branches were generated in random positions (Figures 4H, 4I, and S4M–S4P). These results implied that *GCAM1* functions in the suppression of tissue differentiation and the proliferation of undifferentiated cells that possess the capability to develop into individual thalli when *GCAM1* functions are ectopically induced in the gametophyte.

Orthologous Relationship of *GCAM1* to R2R3-MYBs in Subfamily 14

Gemmae and gemma cups are specialized and derived gametophytic organs for vegetative reproduction in certain Marchantiopsida species, a group of complex thaloid liverworts including *M. polymorpha*. However, homologs of *GCAM1* have been identified across diverse branches of land plants. The inferred amino acid sequence of *GCAM1* contained an R2R3-MYB DNA-binding domain toward the N terminus, and showed the highest similarity (3e–59) to REGULATOR OF AXILLARY MERISTEM 3 (RAX3) in a BLASTP search against the *Arabidopsis thaliana* protein database. Our phylogenetic analysis demonstrated that *GCAM1* belongs to a clade, R2R3-MYB subfamily 14, that is clearly separated from the closest subfamilies including the TDF1 group (Figure 5A). It is also noted that *GCAM1* and the members of R2R3-MYB subfamily 14 share a highly conserved exon-intron structure (Figure 5B). Furthermore, relative to other R2R3-MYB proteins, R2R3-MYB subfamily 14 is characterized by insertion of an additional amino acid between the first and

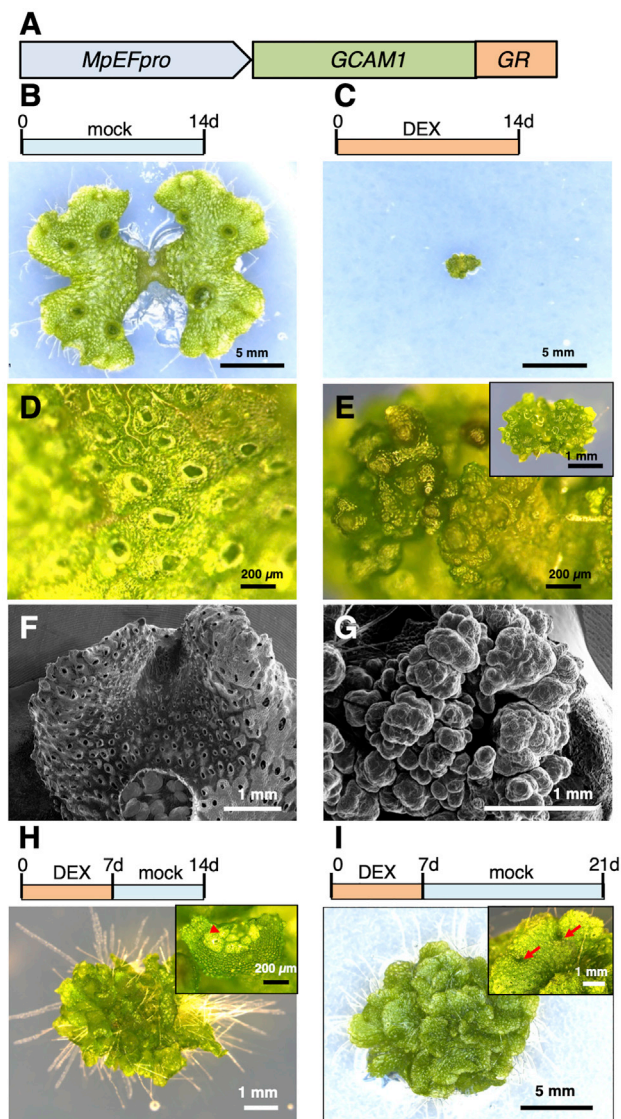


Figure 4. Induction of GCAM1 Function Suppresses Growth and Organ Development in the Thallus of *M. polymorpha*

(A) Schematic representation of the MpEFpro:GCAM1-GR construct.

(B, D, and F) Two-week-old MpEFpro:GCAM1-GR transgenic plant treated with mock. Image of whole thallus (B), and the high-magnification views of the thallus surface by light microscope (D), and scanning electron microscope (F). A number of air pores and air chambers are observed in the thallus surface (D and F).

(C, E, and G) Two-week-old MpEFpro:GCAM1-GR transgenic plant treated with 10 μ M DEX. Image of whole plant (C), and the high-magnification views of the plant by light microscope (E), and scanning electron microscope (G). There is no indication of air chamber development (E and G). Much fewer rhizoids developed from the ventral surface (E, inset).

(H) Two-week-old MpEFpro:GCAM1-GR transgenic plant treated with DEX for the first 7 days and mock for the latter 7 days, and a high-magnification view of the thallus surface (inset). The red arrowhead indicates a developing air chamber.

(I) Three-week-old MpEFpro:GCAM1-GR transgenic plant treated with DEX for the first 7 days and mock for the latter 14 days, and a high-magnification view of the thallus (inset). Red arrows indicate a set of bifurcated apical notches of thalli. See also Figure S4.

second conserved Trp residues of the R2 repeat (4th amino acid back from the second conserved Trp residues) [16], and GCAM1 conforms to this rule (Figure 5C). Comprehensive phylogenetic analysis with all R2R3-MYB transcription factors encoded in several genome-sequenced plant species including *M. polymorpha* has also supported the orthologous relationship of the Marchantia GCAM1 (Mp2R-MYB10: Mapoly0034s0034) to the genes in R2R3-MYB subfamily 14 [12]. These data support strongly the orthologous relationship of GCAM1 to angiosperm proteins in R2R3-MYB subfamily 14. Some angiosperm proteins in R2R3-MYB subfamily 14 are regulatory factors for axillary meristem formation, e.g., *Blind* and *RAX* genes [23–26].

We searched for GCAM1 homologs in other plant species for which transcriptome data are available in the 1KP project [27]. As mentioned above, GCAM1 belongs to R2R3-MYB subfamily 14, which is characterized by an additional amino acid insertion (typically Thr) between the first and second conserved Trp residues of the R2 repeat (Figures 5C and S5E). We located R2R3-MYB genes that have the specific character of subfamily 14 in various liverworts, lycophytes, gymnosperms, and angiosperms, but not in the recently sequenced *Chara braunii* genome [28] nor in the transcriptomes of Zygnematales and Coleochaetales species, which are the extant sister groups of land plants. These data support the emergence of R2R3-MYB subfamily 14 in the common ancestor of land plants, which diverged at least 430 mya [29]. However, we did not identify genes of R2R3-MYB subfamily 14 in the transcriptomic data for mosses and monilophytes, implying secondary loss of R2R3-MYB subfamily 14 in some branches of bryophytes and ferns.

To examine whether *M. polymorpha* GCAM1 is functionally similar to the angiosperm homologs and is able to function in control of axillary meristem formation in angiosperms, we introduced GCAM1 into the *Arabidopsis rax1 rax2 rax3* triple mutant, which exhibits significant inhibition of axillary bud formation compared with the WT [24]. Interestingly, expression of GCAM1 under the control of the *Arabidopsis RAX1* promoter (*RAX1pro:GCAM1*) further inhibited axillary meristem formation in the *rax1 rax2 rax3* triple-mutant background (Figures 5D and S5A–S5D). Given that a non-conserved N-terminal domain is present upstream of (specifically, 28 amino acids from) the R2R3-MYB domain of GCAM1, which is absent in angiosperm R2R3-MYB subfamily 14 members (Figures 5B and 5C), we also tested complementation with a shorter open reading frame (ORF) of GCAM1 (*GCAM1s*), which starts from the second start codon in the original GCAM1 ORF. The *RAX1pro:GCAM1s* transgenic plants showed notable recovery of axillary meristem formation compared with that of the *rax* triple mutant (Figures 5D and S5A–S5D). These results demonstrated the capability of *M. polymorpha* GCAM1 to interact with the genetic machinery of axillary meristem formation in the angiosperm *A. thaliana*.

DISCUSSION

Identification of an Essential Regulator for Vegetative Reproduction in *M. polymorpha*

The basis of vegetative reproduction in seed plants is the *de novo* meristem formation, which allows development of clonal plants. At present, the molecular mechanism of natural vegetative reproduction is poorly known. In the current study, we

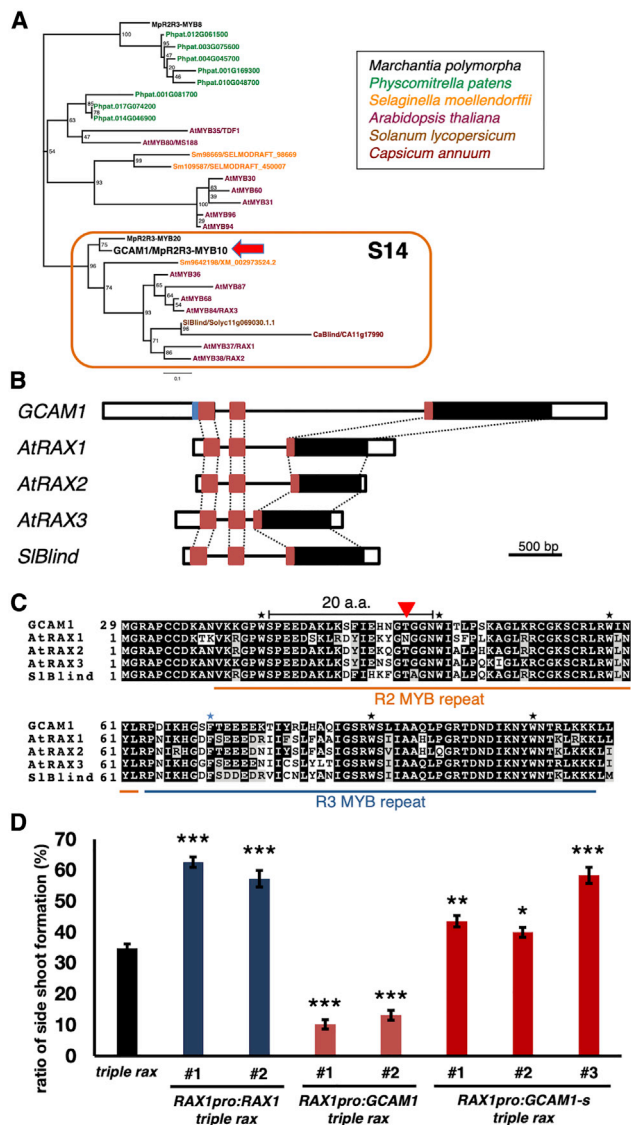


Figure 5. Relationships of GCAM1 and Angiosperm R2R3-MYB Subfamily 14 Orthologs

(A) Phylogenetic analysis of GCAM1 and its homologs in plants. Unrooted maximum-likelihood tree generated from the amino acid sequences for the R2R3-MYB DNA-binding domain of GCAM1 and related R2R3-MYB proteins across diverse plant lineages. The numbers at the nodes are bootstrap values calculated from 1,000 replicates. The scale bar is evolutionary distance as the rate of amino acid substitutions. SIBlind and CaBlind are R2R3-MYB genes reported to function in axillary bud formation in *Solanum lycopersicum* and *Capsicum annuum*, respectively. From *A. thaliana*, not only R2R3-MYBs in subfamily 14 but also other R2R3-MYBs in closely related subfamilies were sampled for the phylogenetic analysis. For *Physcomitrella patens* and *Selaginella moellendorffii*, R2R3-MYBs that showed the eight highest and two highest similarities to GCAM1, respectively, were sampled.

(B) Exon-intron structure of GCAM1, AtRAX1, AtRAX2, AtRAX3, and SIBlind. Box, exon; line, intron; white, 5' or 3' untranslated region. Red and blue boxes indicate R2R3-MYB domains and the non-conserved N-terminal sequence of 28 aa in GCAM1, respectively.

(C) Multiple alignment of R2R3-MYB domains of GCAM1, AtRAX1, AtRAX2, AtRAX3, and SIBlind. Black asterisks indicate conserved Trp residues in plant R2R3-MYBs, and the blue asterisk indicates a Phe residue conserved in R2R3-MYB subfamily 14 [16]. R2R3-MYBs in subfamily 14 are characterized by an aa

identified a key regulator for vegetative reproduction in the basal land plant *M. polymorpha*. Using comprehensive transcriptome analysis and molecular genetic approaches, we identified an R2R3-MYB gene, GCAM1, which is an essential factor for gemma cup development in *M. polymorpha*. Loss-of-function mutants of GCAM1 showed no sign of gemma cup development, but no obvious abnormality was observed in the development of other thallus tissues (Figure 3). This observation suggests that GCAM1 plays a specific role in gemma cup development in the vegetative growth phase of *M. polymorpha*. Our observations on the accumulation of GCAM1 in developing gemma cups and gemmae (Figures 2E–2M) corroborated the suggestion of a specific function for GCAM1 in gemma cup and gemma formation. However, ectopic expression of GCAM1 did not confer excessive production of gemma cups (Figure 4) and instead suppressed organ differentiation and promoted generation of undifferentiated cell clumps (Figures 4 and S4). After GCAM1 induction was halted at 1 week or 2 weeks after DEX treatment, numerous thalli developed directly from the cell clumps (Figure 4), suggesting that the cell clumps consist of cells with the potential to differentiate into meristematic apical cells of the thallus. These results suggest that GCAM1 might function to suppress tissue differentiation and maintain the undifferentiated status of cells in the gametophyte, which may be essential for the floor cells of the gemma cup to form gemma initials. The role of GCAM1 would be to proliferate floor cells of gemma cups and to maintain the low differentiation level of these cells, which may be a prerequisite for gemma cup development and gemma initiation. Given that GCAM1 expression was observed not only in the floor cells of the gemma cup but also in the developing gemmae, GCAM1 may also perform a critical role in gemma differentiation. In gemma development, a gemma initial cell sequentially divides into a flat multicellular body, and two apical meristems are established on opposite sides of the disk [7]. Thus, gemma development can be considered to be a process similar to meristem formation. We surmise that the GCAM1 function to maintain the undifferentiated status of cells would be important for proper gemma development. Alternatively, GCAM1 may have different roles in gemma initiation and gemma differentiation. In stoma differentiation of angiosperms, the bHLH transcription factors SCRM/ICE1 and SCRM2 act throughout the different stages of stomatal development by changing their interaction partners

insertion compared with other R2R3-MYB subfamilies between the first and the second Trp residues of the R2 repeat, the position of which is indicated by the red triangle.

(D) Genetic complementation of the *Arabidopsis rax1-3 rax2-1 rax3-1* mutant with *Arabidopsis RAX1* and *Marchantia GCAM1* (see Figure S5 for details). Lateral shoot formation in rosette leaf axils of the *rax1-3 rax2-1 rax3-1* mutant (*triple rax*; $n = 30$), two independent transformants containing *RAX1*-promoter-driven *RAX1* open reading frame (ORF1) in the *rax* triple-mutant background (*RAX1pro:RAX1 triple rax*; $n = 15$), two independent transformants containing the *RAX1*-promoter-driven GCAM1 ORF in the *rax* triple-mutant background (*RAX1pro:GCAM1 triple rax*; $n = 15$), and three independent transgenics containing the *RAX1*-promoter-driven shorter version of the GCAM1 ORF in the *rax* triple-mutant background (*RAX1pro:GCAM1s triple rax*, $n = 15$). Values represent means \pm SE. Asterisks indicate significant differences relative to the *triple-rax* mutant (Student's *t* test, * $p < 0.05$, ** $p < 0.02$, *** $p < 0.0001$). See also Figure S5 and Data S2.

SPCH, MUTE, and FAMA [30]. Similarly, GCAM1 may interact with different partners to control different sets of genes during gemma differentiation.

The Orthologous Relationship of GCAM1 to the Regulatory Factors for Axillary Meristem Formation in Angiosperms

The present phylogenetic analysis indicated that GCAM1 is orthologous to angiosperm genes in R2R3-MYB subfamily 14 [16], which include regulatory factors for axillary meristem formation, e.g., tomato *Blind* and *Arabidopsis RAX* genes [23–26] (Figure 5A). Interspecific complementation analyses demonstrated that *M. polymorpha* GCAM1 can interact with the genetic machinery of axillary meristem formation in *Arabidopsis* (Figure 5D). These results imply that similar mechanisms control vegetative reproduction in the gametophyte body of the liverwort *M. polymorpha* and axillary meristem formation in the sporophyte body of angiosperms. In *Arabidopsis*, RAX1 and RAX3 are specifically expressed in the boundary region and axils and between the SAM and leaf primordia, and regulate axillary meristem formation during vegetative development [24, 25]. In angiosperms, boundary zones are characterized by a lower rate of cell division and lower concentrations of auxin and brassinosteroids than those of leaf primordia, resulting in a low degree of differentiation of boundary cells that exhibit higher competence for meristem formation [2, 31]. In *Arabidopsis*, CUP-SHAPED COTYLEDON genes (CUCs) are also known to be expressed in boundary zones and required for boundary formation [2]. The tomato gene *Goblet*, which is the tomato ortholog of CUCs, promotes shoot formation at the leaflet boundary, suggesting that the specification of the boundary zone is the common basis of axillary bud formation and vegetative reproduction in angiosperms [32]. The cells of the gemma cup floor in the liverwort *M. polymorpha*, in which the ability to regenerate clonal plantlets is maintained, could be considered to show similar characteristics to cells in the boundary zones of angiosperms.

We speculate that such an R2R3-MYB-mediated regulatory mechanism for the establishment and maintenance of cell groups showing a low differentiation level, but retaining the competence to generate meristematic cells, was acquired in the common ancestor of land plants. In the course of land plant evolution, such a regulatory mechanism was co-opted for diverse developmental processes, such as vegetative reproduction in Marchantiales species and axillary bud formation in angiosperms.

Further investigation of the GCAM1-mediated gene regulatory network in *M. polymorpha* and comparison with that for axillary meristem formation in angiosperms should shed light on the conservation or diversification of regulatory mechanisms for proliferation of meristems in land plants.

STAR★METHODS

Detailed methods are provided in the online version of this paper and include the following:

- KEY RESOURCES TABLE
- LEAD CONTACT AND MATERIALS AVAILABILITY
- EXPERIMENTAL MODEL AND SUBJECT DETAILS
 - Plant material and growth conditions

METHOD DETAILS

- RNA extraction and Illumina sequencing
- RNA-seq data analysis
- Quantitative RT-PCR analysis
- Generation of transformants for promoter-reporter analysis
- Generation of *gcam1*^{ko} and GCAM1-Citrine knock-in plants
- CRISPR/Cas9-based genome editing of GCAM1
- Visualization of GCAM1-Citrine
- Histology and light microscopy
- Generation of GCAM1-overexpressing plants
- Phenotypic analysis of MpEFpro:GCAM1-GR plants
- Phylogenetic analysis of GCAM1
- Multiple alignment of GCAM1 and related homologs in diverse land plants
- Introduction of GCAM1 into an *Arabidopsis rax* triple mutant

QUANTIFICATION AND STATISTICAL ANALYSIS

DATA AND CODE AVAILABILITY

SUPPLEMENTAL INFORMATION

Supplemental Information can be found online at <https://doi.org/10.1016/j.cub.2019.10.004>.

ACKNOWLEDGMENTS

The authors thank John L. Bowman and Eduardo Flores-Sandoval (Monash University, Australia) for critical reading of the manuscript; Andrea Busch, Sabine Zachgo (University of Osnabrück, Germany), Shohei Yamaoka, and members of T. Kohchi's laboratory for technical assistance and discussions; and Naho Maehara for illustration of the graphical abstract. The authors thank Ursula Pfordt and Alexandra Kalde for excellent technical assistance. Research in the Theres laboratory was supported by the Max Planck Society. The RNA-seq analysis was supported by NIBB Collaborative Research Program grant 15-823 (K.I.). This study was funded by MEXT KAKENHI grants 18H04836 (R.N.), 25113009 (T.K.), 25119711, 15H01233, and 17H06472 (K.I.); JSPS KAKENHI grants 15H04391, 19H03247 (K.I.), and 19K16167 (Y.Y.); and the SUNTORY Foundation for Life Sciences, Yamada Science Foundation, and Asahi Glass Foundation (K.I.). We thank Robert McKenzie, PhD, from the Edanz Group (<https://www.edanzediting.com/ac>) for editing a draft of this manuscript.

AUTHOR CONTRIBUTIONS

K.I., S.T., and Y.Y. designed the research; S.T., Y.Y., T.S., R.N., Q.W., H.K., K.T., and K.I. performed the research; Y.Y., S.T., R.N., Q.W., K.T.Y., H.K., K.T., H.F., T.M., T.K., and K.I. analyzed the data; and K.I. and Y.Y. wrote the paper.

DECLARATION OF INTERESTS

The authors declare no competing interests.

Received: March 26, 2019

Revised: August 16, 2019

Accepted: October 2, 2019

Published: November 7, 2019

REFERENCES

1. Steeves, T.A., and Sussex, I.M. (1989). *Patterns in Plant Development, Second Edition* (Cambridge University Press).

2. Wang, Q., Hasson, A., Rossmann, S., and Theres, K. (2016). Divide et impera: boundaries shape the plant body and initiate new meristems. *New Phytol.* *209*, 485–498.
3. Steward, F.C., Mapes, M.O., Kent, A.E., and Holsten, R.D. (1964). Growth and development of cultured plant cells. *Science* *143*, 20–27.
4. Steward, F.C., Mapes, M.O., and Mears, K. (1958). Growth and organized development of cultured cells. II. Organization in cultures grown from freely suspended cells. *Am. J. Bot.* *45*, 705–708.
5. Klimesová, J., and Klimeš, L. (2007). Bud banks and their role in vegetative regeneration—a literature review and proposal for simple classification and assessment. *Perspect. Plant Ecol. Evol. Syst.* *8*, 115–129.
6. Davis, F.T., Geneve, R.L., Wilson, S.E., Hartmann, H.T., and Kester, D.E. (2017). *Hartmann & Kester's Plant Propagation: Principles and Practices* (Pearson).
7. Shimamura, M. (2016). *Marchantia polymorpha*: taxonomy, phylogeny and morphology of a model system. *Plant Cell Physiol.* *57*, 230–256.
8. Barnes, C.R., and Land, W.J.G. (1908). Bryological papers. II. The origin of the cupule of *Marchantia*. *Bot. Gaz.* *46*, 401–409.
9. Voth, P.D., and Hamner, K.C. (1940). Responses of *Marchantia polymorpha* to nutrient supply and photoperiod. *Bot. Gaz.* *102*, 169–205.
10. Voth, P.D. (1941). Gemmae-cup production in *Marchantia polymorpha* and its response to calcium deficiency and supply of other nutrients. *Bot. Gaz.* *103*, 310–325.
11. Benson-Evans, K. (1964). Physiology of the reproduction of bryophytes. *Bryologist* *67*, 431–445.
12. Bowman, J.L., Kohchi, T., Yamato, K.T., Jenkins, J., Shu, S., Ishizaki, K., Yamaoka, S., Nishihama, R., Nakamura, Y., Berger, F., et al. (2017). Insights into land plant evolution garnered from the *Marchantia polymorpha* genome. *Cell* *171*, 287–304.e15.
13. Ishizaki, K., Nishihama, R., Yamato, K.T., and Kohchi, T. (2016). Molecular genetic tools and techniques for *Marchantia polymorpha* research. *Plant Cell Physiol.* *57*, 262–270.
14. Ishizaki, K. (2017). Evolution of land plants: insights from molecular studies on basal lineages. *Biosci. Biotechnol. Biochem.* *81*, 73–80.
15. Pires, N.D., and Dolan, L. (2012). Morphological evolution in land plants: new designs with old genes. *Philos. Trans. R. Soc. Lond. B Biol. Sci.* *367*, 508–518.
16. Stracke, R., Werber, M., and Weisshaar, B. (2001). The R2R3-MYB gene family in *Arabidopsis thaliana*. *Curr. Opin. Plant Biol.* *4*, 447–456.
17. Bowman, J.L., Araki, T., Arteaga-Vazquez, M.A., Berger, F., Dolan, L., Haseloff, J., Ishizaki, K., Kyoizuka, J., Lin, S.S., Nagasaki, H., et al. (2016). The naming of names: guidelines for gene nomenclature in *Marchantia*. *Plant Cell Physiol.* *57*, 257–261.
18. Ishizaki, K., Johzuka-Hisatomi, Y., Ishida, S., Iida, S., and Kohchi, T. (2013). Homologous recombination-mediated gene targeting in the liverwort *Marchantia polymorpha* L. *Sci. Rep.* *3*, 1532.
19. Sugano, S.S., Shirakawa, M., Takagi, J., Matsuda, Y., Shimada, T., Hara-Nishimura, I., and Kohchi, T. (2014). CRISPR/Cas9-mediated targeted mutagenesis in the liverwort *Marchantia polymorpha* L. *Plant Cell Physiol.* *55*, 475–481.
20. Sugano, S.S., Nishihama, R., Shirakawa, M., Takagi, J., Matsuda, Y., Ishida, S., Shimada, T., Hara-Nishimura, I., Osakabe, K., and Kohchi, T. (2018). Efficient CRISPR/Cas9-based genome editing and its application to conditional genetic analysis in *Marchantia polymorpha*. *PLoS ONE* *13*, e0205117.
21. Lloyd, A.M., Schena, M., Walbot, V., and Davis, R.W. (1994). Epidermal cell fate determination in *Arabidopsis*: patterns defined by a steroid-inducible regulator. *Science* *266*, 436–439.
22. Schena, M., Lloyd, A.M., and Davis, R.W. (1991). A steroid-inducible gene expression system for plant cells. *Proc. Natl. Acad. Sci. USA* *88*, 10421–10425.
23. Schmitz, G., Tillmann, E., Carriero, F., Fiore, C., Cellini, F., and Theres, K. (2002). The tomato Blind gene encodes a MYB transcription factor that controls the formation of lateral meristems. *Proc. Natl. Acad. Sci. USA* *99*, 1064–1069.
24. Müller, D., Schmitz, G., and Theres, K. (2006). Blind homologous R2R3 Myb genes control the pattern of lateral meristem initiation in *Arabidopsis*. *Plant Cell* *18*, 586–597.
25. Keller, T., Abbott, J., Moritz, T., and Doerner, P. (2006). *Arabidopsis* REGULATOR OF AXILLARY MERISTEMS1 controls a leaf axil stem cell niche and modulates vegetative development. *Plant Cell* *18*, 598–611.
26. Jeifetz, D., David-Schwartz, R., Borovsky, Y., and Paran, I. (2011). CaBLIND regulates axillary meristem initiation and transition to flowering in pepper. *Planta* *234*, 1227–1236.
27. Matasci, N., Hung, L.H., Yan, Z., Carpenter, E.J., Wickett, N.J., Mirarab, S., Nguyen, N., Warnow, T., Ayyampalayam, S., Barker, M., et al. (2014). Data access for the 1,000 plants (1KP) project. *Gigascience* *3*, 17.
28. Nishiyama, T., Sakayama, H., de Vries, J., Buschmann, H., Saint-Marcoux, D., Ullrich, K.K., Haas, F.B., Vanderstraeten, L., Becker, D., Lang, D., et al. (2018). The Chara genome: secondary complexity and implications for plant terrestrialization. *Cell* *174*, 448–464.e24.
29. Morris, J.L., Puttick, M.N., Clark, J.W., Edwards, D., Kenrick, P., Pressell, S., Wellman, C.H., Yang, Z., Schneider, H., and Donoghue, P.C.J. (2018). The timescale of early land plant evolution. *Proc. Natl. Acad. Sci. USA* *115*, E2274–E2283.
30. Kanaoka, M.M., Pillitteri, L.J., Fujii, H., Yoshida, Y., Bogenschutz, N.L., Takabayashi, J., Zhu, J.K., and Torii, K.U. (2008). SCREAM/ICE1 and SCREAM2 specify three cell-state transitional steps leading to *Arabidopsis* stomatal differentiation. *Plant Cell* *20*, 1775–1785.
31. Wang, Q., Kohlen, W., Rossmann, S., Vernoux, T., and Theres, K. (2014). Auxin depletion from the leaf axil conditions competence for axillary meristem formation in *Arabidopsis* and tomato. *Plant Cell* *26*, 2068–2079.
32. Rossmann, S., Kohlen, W., Hasson, A., and Theres, K. (2015). Lateral suppressor and Goble act in hierarchical order to regulate ectopic meristem formation at the base of tomato leaflets. *Plant J.* *81*, 837–848.
33. Gamborg, O.L., Miller, R.A., and Ojima, K. (1968). Nutrient requirements of suspension cultures of soybean root cells. *Exp. Cell Res.* *50*, 151–158.
34. Nystedt, B., Street, N.R., Wetterbom, A., Zuccolo, A., Lin, Y.C., Scofield, D.G., Vezzi, F., Delhomme, N., Giacomello, S., Alexeyenko, A., et al. (2013). The Norway spruce genome sequence and conifer genome evolution. *Nature* *497*, 579–584.
35. Ishizaki, K., Chiyoda, S., Yamato, K.T., and Kohchi, T. (2008). *Agrobacterium*-mediated transformation of the haploid liverwort *Marchantia polymorpha* L., an emerging model for plant biology. *Plant Cell Physiol.* *49*, 1084–1091.
36. Ishizaki, K., Nishihama, R., Ueda, M., Inoue, K., Ishida, S., Nishimura, Y., Shikanai, T., and Kohchi, T. (2015). Development of Gateway binary vector series with four different selection markers for the liverwort *Marchantia polymorpha*. *PLoS ONE* *10*, e0138876.
37. Yamaoka, S., Nishihama, R., Yoshitake, Y., Ishida, S., Inoue, K., Saito, M., Okahashi, K., Bao, H., Nishida, H., Yamaguchi, K., et al. (2018). Generative cell specification requires transcription factors evolutionarily conserved in land plants. *Curr. Biol.* *28*, 479–486.e5.
38. Überlacker, B., and Werr, W. (1996). Vectors with rare-cutter restriction enzyme sites for expression of open reading frames in transgenic plants. *Mol. Breed.* *2*, 293–295.
39. Papadopoulos, J.S., and Agarwala, R. (2007). COBALT: constraint-based alignment tool for multiple protein sequences. *Bioinformatics* *23*, 1073–1079.
40. Edgar, R.C. (2004). MUSCLE: multiple sequence alignment with high accuracy and high throughput. *Nucleic Acids Res.* *32*, 1792–1797.
41. Gouy, M., Guindon, S., and Gascuel, O. (2010). SeaView version 4: a multi-platform graphical user interface for sequence alignment and phylogenetic tree building. *Mol. Biol. Evol.* *27*, 221–224.
42. Guindon, S., Dufayard, J.F., Lefort, V., Anisimova, M., Hordijk, W., and Gascuel, O. (2010). New algorithms and methods to estimate

- maximum-likelihood phylogenies: assessing the performance of PhyML 3.0. *Syst. Biol.* 59, 307–321.
43. Kim, D., Pertea, G., Trapnell, C., Pimentel, H., Kelley, R., and Salzberg, S.L. (2013). TopHat2: accurate alignment of transcriptomes in the presence of insertions, deletions and gene fusions. *Genome Biol.* 14, R36.
 44. Trapnell, C., Roberts, A., Goff, L., Pertea, G., Kim, D., Kelley, D.R., Pimentel, H., Salzberg, S.L., Rinn, J.L., and Pachter, L. (2012). Differential gene and transcript expression analysis of RNA-seq experiments with TopHat and Cufflinks. *Nat. Protoc.* 7, 562–578.
 45. Xiao, A., Cheng, Z., Kong, L., Zhu, Z., Lin, S., Gao, G., and Zhang, B. (2014). CasOT: a genome-wide Cas9/gRNA off-target searching tool. *Bioinformatics* 30, 1180–1182.
 46. Chiyoda, S., Ishizaki, K., Kataoka, H., Yamato, K.T., and Kohchi, T. (2008). Direct transformation of the liverwort *Marchantia polymorpha* L. by particle bombardment using immature thalli developing from spores. *Plant Cell Rep.* 27, 1467–1473.
 47. Kubota, A., Ishizaki, K., Hosaka, M., and Kohchi, T. (2013). Efficient *Agrobacterium*-mediated transformation of the liverwort *Marchantia polymorpha* using regenerating thalli. *Biosci. Biotechnol. Biochem.* 77, 167–172.
 48. Sugano, S.S., and Nishihama, R. (2018). CRISPR/Cas9-based genome editing of transcription factor genes in *Marchantia polymorpha*. *Methods Mol. Biol.* 1830, 109–126.
 49. Jin, J., Tian, F., Yang, D.C., Meng, Y.Q., Kong, L., Luo, J., and Gao, G. (2017). PlantTFDB 4.0: toward a central hub for transcription factors and regulatory interactions in plants. *Nucleic Acids Res.* 45, D1040–D1045.
 50. Raman, S., Greb, T., Peaucelle, A., Blein, T., Laufs, P., and Theres, K. (2008). Interplay of miR164, CUP-SHAPED COTYLEDON genes and LATERAL SUPPRESSOR controls axillary meristem formation in *Arabidopsis thaliana*. *Plant J.* 55, 65–76.

STAR★METHODS

KEY RESOURCES TABLE

REAGENT or RESOURCE	SOURCE	IDENTIFIER
Bacterial and Virus Strains		
<i>Escherichia coli</i> DH5 α	Widely distributed	N/A
<i>Agrobacterium tumefaciens</i> GV2260	Widely distributed	N/A
Chemicals, Peptides, and Recombinant Proteins		
Gamborg's B5 salts	[33]	N/A
Murashige-Skoog salts	Wako Pure Chemical Industries	Cat#392-00591
Hygromycin B	Nacalai Tesque	Cat#07296-24
cefotaxime (CLAFORAN)	Sanofi	Cat#6132409D1050
dexamethasone (DEX)	Sigma-Aldrich	Cat#D4902
Critical Commercial Assays		
Technovit 7100 combipack	Kulzer Technique	Cat#64709003
RNeasy Plant Mini kit	QIAGEN	Cat#74904
Bioanalyzer RNA6000 Nano Kit	Agilent Technologies	Cat#5067-1511
TruSeq RNA Sample Prep Kit v.2	Illumina	Cat#FS-122-2001
High Sensitivity DNA kit	Agilent Technologies	Cat#5067-4626
KAPA Library Quantification Kit	NIPPON Genetics	Cat#KK4828
KOD FX Neo DNA polymerase	Toyobo Life Science	Cat#KFX-201
KOD -Plus- Neo DNA polymerase	Toyobo Life Science	Cat#KFX-401
pENTR/D-TOPO Cloning Kit	Thermo Fisher Scientific	Cat#K240020
Gateway LR clonase II Enzyme mix	Thermo Fisher Scientific	Cat#11790120
RNAlater	Thermo Fisher Scientific	Cat#AM7020
ReverTra Ace qPCR RT Master Mix with gDNA remover	TOYOBO	Cat#FSQ-301
KOD SYBR qRT-PCR Mix	TOYOBO	Cat#QKD-201
<i>PacI</i>	New England Biolabs	Cat#R0547S
<i>AscI</i>	New England Biolabs	Cat#R0558S
<i>SbfI</i>	New England Biolabs	Cat# R0642S
<i>SacI</i>	New England Biolabs	Cat# R0156S
<i>AvrII</i>	New England Biolabs	Cat# R0174S
Deposited Data		
<i>Marchantia polymorpha</i> transcriptome data	This paper	DDBJ: DRA005912
<i>Marchantia polymorpha</i> genome v.3.1	[12]	http://marchantia.info
<i>Arabidopsis thaliana</i> genome TAIR10	TAIR	https://www.arabidopsis.org/
<i>Physcomitrella patens</i> v3.0	Phytozome	https://phytozome.jgi.doe.gov/pz/portal.html ; RRID: SCR_006507
<i>Selaginella moellendorffii</i> genome v.1.0	Phytozome	https://phytozome.jgi.doe.gov/pz/portal.html ; RRID: SCR_006507
<i>Solanum lycopersicum</i> Blind amino acid sequence	[23]	Genbank: AAL69334
<i>Capsicum annuum</i> CaBLIND amino acid sequence	[26]	Genbank: JF496586
<i>Picea abies</i> genome	[34]	http://congenie.org/start
Transcriptome data generated by 1000 Plant (1KP) project	[27]	https://db.cngb.org/datamart/plant/DATApla4/
Experimental Models: Organisms/Strains		
<i>Marchantia polymorpha</i> Tak-1	[35]	N/A
<i>Marchantia polymorpha</i> Tak-2	[35]	N/A
<i>Marchantia polymorpha</i> <i>gcam1</i> ^{ko}	this paper	N/A
<i>Marchantia polymorpha</i> <i>GCAM1-Citrine knock-in</i>	this paper	N/A

(Continued on next page)

Continued

REAGENT or RESOURCE	SOURCE	IDENTIFIER
<i>Marchantia polymorpha</i> GCAM1pro:GUS	this paper	N/A
<i>Marchantia polymorpha</i> MpEFpro:GCAM1	this paper	N/A
<i>Marchantia polymorpha</i> MpEFpro:GCAM1-GR	this paper	N/A
<i>Arabidopsis thaliana</i> triple rax	[24]	N/A
<i>Arabidopsis thaliana</i> RAX1pro:RAX1 triple rax	this paper	N/A
<i>Arabidopsis thaliana</i> RAX1pro:GCAM1 triple rax	this paper	N/A
<i>Arabidopsis thaliana</i> RAX1pro:GCAM1s triple rax	this paper	N/A
Oligonucleotides		
See Table S3	this paper	N/A
Recombinant DNA		
pMpGWB103	[36]	GenBank: LC057445
pMpGWB104	[36]	GenBank: LC057446
pMpGWB313	[36]	GenBank: LC057529
pJHY-TMp1	[18]	N/A
pJHY-TMp1-Cit	[37]	N/A
pMpGE_En01	[20]	GenBank: LC090754
pMpGE011	[20]	GenBank: LC090757
pGPTV-BAR-Ascl	[38]	N/A
Software and Algorithms		
COBALT	[39]	https://www.ncbi.nlm.nih.gov/tools/cobalt/
MUSCLE	[40]	https://www.ebi.ac.uk/Tools/msa/muscle/
SeaView	[41]	http://doua.prabi.fr/software/seaview
PhyML 3.0	[42]	http://www.atgc-montpellier.fr/phyml/
TopHat ver 2.1.1	[43]	http://ccb.jhu.edu/software/tophat/index.shtml
Cuffdiff 2.2.1	[44]	http://cole-trapnell-lab.github.io/cufflinks/
CasOT	[45]	https://omictools.com/casot-tool

LEAD CONTACT AND MATERIALS AVAILABILITY

Further information and requests for resources and reagents should be directed to and will be fulfilled by the Lead Contact, Kimitsune Ishizaki (kimi@emerald.kobe-u.ac.jp). Please note that the transfer of transgenic plants will be subject to MTA and any relevant import permits.

EXPERIMENTAL MODEL AND SUBJECT DETAILS**Plant material and growth conditions**

Male and female accessions of *M. polymorpha*, Takaragaike-1 (Tak-1) and Takaragaike-2 (Tak-2), respectively [35], were maintained asexually. F₁ spores generated by crossing Tak-2 and Tak-1 were used for generation of *gcam1^{ko}* and *GCAM1-Citrine* knock-in plants. Formation of sexual organs was induced by far-red irradiation as described previously [46]. Mature sporangia were collected 3–4 weeks after crossing, air-dried for 7–10 days, and stored at –80°C until use.

Marchantia polymorpha plants were cultured using half-strength Gamborg's B5 medium [33] containing 1% agar under 50–60 μmol photons m⁻² s⁻¹ continuous white light with a cold cathode fluorescent lamp (OPT-40C-N-L; Optrom, Miyagi, Japan) or light-emitting diode (VGL-1200W; SYNERGYTEC, Tokushima, Japan) at 22°C unless otherwise defined.

METHOD DETAILS**RNA extraction and Illumina sequencing**

Developing gemma cups located within 3 mm from an apical notch of 3-week-old thalli were manually dissected and immediately immersed in RNAlater (Thermo Fisher Scientific, Waltham, MA, USA). For the control, the midrib region between gemma cups of 3-week-old thalli and 1-week-old thalli, which had no visible gemma cups, were also sampled. The collected samples were divided into three pools for extraction of total RNA.

Total RNA was extracted with the RNeasy Plant Mini Kit (QIAGEN) in accordance with the manufacturer's protocol. The quality and quantity of resultant total RNA were evaluated using a NanoDrop 1000 spectrophotometer (Thermo Fisher Scientific), Qubit 2.0 Fluorometer (Thermo Fisher Scientific), and a Bioanalyzer RNA6000 Nano Kit (Agilent Technologies, Santa Clara, CA, USA). The sequence libraries were constructed with a TruSeq RNA Sample Prep Kit v2 (Illumina, San Diego, CA, USA) in accordance with the manufacturer's protocol. The quality and quantity of each library were determined using a Bioanalyzer with High Sensitivity DNA kit (Agilent Technologies), and KAPA Library Quantification Kit for Illumina (Nippon Genetics). Equal amounts of each library were mixed to make the 2 nM pooled library. Illumina sequencing was performed using a HiSeq 2000 platform (Illumina) to produce 101 single-end data. All reads obtained have been deposited in the DDBJ and are available through the Sequence Read Archive (SRA) under the accession number DRA005912.

RNA-seq data analysis

The resultant reads were mapped to the draft genome of *M. polymorpha* version 3.1 by TopHat ver 2.1.1 [43] with the default parameters. To identify differentially expressed genes (DEGs), the mapped reads from different samples were compared by Cuffdiff 2.2.1 [44] using the default parameters and transcript annotation generated on the *Marchantia* genome assembly ver. 3.1 [12]. Among DEGs, genes with a log₂-fold change > 1 were considered as preferentially expressed in the gemma cup (for details, see [Data S1A–S1C](#)). The supercomputers of the Academic Center for Computing and Media Studies at Kyoto University and of the Computing Center at the Faculty of Biology-Oriented Science and Technology, Kindai University were used for computation.

Quantitative RT-PCR analysis

One microgram of total RNA was reverse-transcribed in a 20 μ L reaction mixture using ReverTra Ace qPCR RT Master Mix with gDNA remover (TOYOBO). After the reaction, the cDNA samples were diluted with 220 μ L distilled water and 2 μ L aliquots were amplified with the LightCycler Nano Real-time PCR Detection System (Roche Applied Science, Tokyo, Japan) using the KOD SYBR qRT-PCR Mix (TOYOBO). The PCR cycling program was performed in accordance with the manufacturer's protocol. The primers used in these experiments are listed in [Table S3](#). MpEF1 α was used as an internal control.

Generation of transformants for promoter-reporter analysis

To construct *GCAM1pro:GUS*, the *GCAM1* genomic region, including a 5593-bp fragment upstream of the 83rd Arg codon in the second exon, was amplified from Tak-1 genomic DNA by PCR with the primers GCAM1pro_L1 and GCAM1pro_R2 and cloned into the pENTR/D-TOPO cloning vector (Life Technologies, Rockville, MD, USA). This entry vector was used in the Gateway LR reaction (Life Technologies) with the Gateway binary vector pMpGWB104 [36] to generate the *GCAM1pro:GUS* binary construct, in which the *GUS* reporter gene was translationally fused at the middle of the second exon of *GCAM1*. The *GCAM1pro:GUS* vectors were introduced into regenerating thalli of Tak-1 by *Agrobacterium*-mediated transformation as previously described [47]. Transformants were selected with 10 μ g/ml hygromycin B and 100 μ g/ml cefotaxime.

Generation of *gcam1*^{ko} and *GCAM1*-Citrine knock-in plants

For knock-in and knock-out experiments, Tak-1 genomic sequences were amplified by PCR with KOD FX Neo DNA polymerase (TOYOBO) and the primer pair listed in [Table S3](#). The amplified products were inserted into the *PacI* and *Ascl* sites of pJHY-TMp1 [18] and pJHY-TMp1-Cit [37] to generate *gcam1*^{ko} and *GCAM1*-Citrine transformants, respectively. The vectors were introduced into germinating spores via *Agrobacterium tumefaciens* GV2260 as described previously [18]. Transformants were selected with 10 μ g/ml hygromycin B and 100 μ g/ml cefotaxime. The transformants harboring the targeted insertions were selected by PCR with KOD FX Neo DNA polymerase and the primer pairs listed in [Table S3](#) and [Figure S2](#).

CRISPR/Cas9-based genome editing of *GCAM1*

Loss-of-function mutants of *GCAM1* were generated with the CRISPR/Cas9 system as described previously [20, 48]. We selected two target sequences, one located in the first exon, and the other located in the second exon of *GCAM1* ([Figure S4](#)). An off-target search was performed using casOT [45]. Synthetic oligo DNAs for respective target sites shown in [Table S3](#) were annealed, inserted into the entry vector pMpGE_En01, and then introduced into the destination vector pMpGE011 [20, 48]. The vectors were introduced into regenerating thalli of Tak-1 via *A. tumefaciens* GV2260 [47], and transformants were selected with 0.5 μ M chlorsulfuron. Genomic DNA was isolated from transformants and amplified from the target region by PCR. The PCR product was used for sequencing of the respective target sites with an ABI 3100 genetic analyzer (Applied Biosystems, Foster City, CA, USA).

Visualization of *GCAM1*-Citrine

Transverse sections of *GCAM1*-Citrine knock-in thalli with apical notches were generated with a pair of razors, and observed under a confocal laser scanning microscope (Olympus FLUOVIEW FV1000, Tokyo, Japan). Excitation and emission wavelengths for Citrine fluorescence were 515 nm (Ar laser) and 520–570 nm, respectively.

Histology and light microscopy

For histochemical GUS staining, *GCAM1pro:GUS* plants were grown on half-strength B5 medium for respective periods under continuous white light. GUS staining was performed as described previously and at least five independent lines were observed

for GUS staining patterns using S8APO (Leica Microsystems) and DMS1000 (Leica) stereoscopic microscopes, or an upright light microscope Axio Scope.A1 (Zeiss) equipped with an AxioCam ERc5c camera (Zeiss).

For plastic-embedded sectioning, 3-week-old thalli developed from gemmae were dissected into small pieces and transferred to fixative solution (2% glutaraldehyde in 0.05 M phosphate buffer, pH 7.0), evacuated with a water aspirator until the specimens sank, and fixed for 2 days at room temperature. The samples were dehydrated in a graded ethanol series and embedded in Technovit 7100 plastic resin. Semi-thin sections (5 μm thickness) for light microscopy were obtained with a microtome (HM 335E, Leica Microsystems, Heerbrugg, Switzerland) and stained with toluidine blue O.

For scanning electron microscopy, plant samples were frozen in liquid nitrogen and directly observed on a VHX-D500 microscope (KEYENCE, Osaka, Japan).

Generation of GCAM1-overexpressing plants

To generate *MpEFpro:GCAM1*, the *GCAM1* coding sequence was amplified by PCR using KOD Plus Neo DNA polymerase (TOYOBO) with the primer set GCAM1-cds-L1/GCAM1-cds-sR and cloned into the pENTR/D-TOPO cloning vector. The entry vector was used in the Gateway LR reaction with the Gateway binary vector pMpGWB103 [36]. The *MpEFpro:GCAM1* vector was introduced into regenerating thalli of Tak-1 as previously described [47]. Transformants were selected with 10 $\mu\text{g/ml}$ hygromycin B and 100 $\mu\text{g/ml}$ cefotaxime.

To construct *MpEFpro:GCAM1-GR*, the *GCAM1* CDS was amplified by PCR using KOD Plus Neo DNA polymerase (TOYOBO) with the primer set GCAM1-cds-L1/GCAM1-cds-nsR and cloned into the pENTR/D-TOPO cloning vector. The entry vector was used in the Gateway LR reaction with the Gateway binary vector pMpGWB313 [36]. The *MpEFpro:GCAM1-GR* vector was introduced into regenerating thalli of Tak-1 as previously described [47]. Transformants were selected with 0.5 μM chlorsulfuron and 100 $\mu\text{g/ml}$ cefotaxime.

The transformants and mutants were named consistent with the nomenclatural rules for *M. polymorpha* [17].

Phenotypic analysis of MpEFpro:GCAM1-GR plants

In the vegetative phase, DEX treatment of *MpEFpro:GCAM1-GR* plants was performed by culture in half-strength Gamborg's B5 medium containing 10 μM DEX or applying 200 μL of 10 μM DEX solution to plants.

Phylogenetic analysis of GCAM1

For phylogenetic analysis of GCAM1 and related homologous R2R3-MYBs, sequence information was obtained from the PlantTFDB [49] and Phytozome databases. A multiple alignment of amino acid sequences of GCAM1 and homologous R2R3-MYBs was first constructed using COBALT [39] and then using the MUSCLE program [40] implemented in SeaView version 4.5.4 [41] with the default parameters. The alignment is available as [Data S2](#). The conserved region covering the R2R3-MYB domain was extracted before phylogenetic tree construction, which was performed using the maximum likelihood method with PhyML [42] with the LG substitution model. A bootstrap analysis with 1000 replicates was performed in each analysis to assess statistical support for the topology. The phylogenetic tree was visualized using FigTree (<http://tree.bio.ed.ac.uk/software/figtree/>).

Multiple alignment of GCAM1 and related homologs in diverse land plants

Homologs of GCAM1 were searched and obtained from Phytozome databases, *Picea abies* genome [34], and transcriptome data generated by 1000 Plant (1KP) project [27]. A multiple alignment of amino acid sequences of GCAM1 and homologous R2R3-MYBs was constructed using the MUSCLE program [40].

Introduction of GCAM1 into an Arabidopsis rax triple mutant

To generate a RAX1 promoter construct, the upstream region of *Arabidopsis RAX1* including the promoter and 5' untranslated region (2939 bp) were amplified by PCR using the primers Myb37-pro-SbfIF and Myb37-pro-AscIR. The resulting PCR fragment was inserted into the *SbfI* and *AscI* sites of the pGPTV-BAR-*AscI* vector [38] in front of the *GUS* gene (Vector pFY124). A GFP fragment was amplified using the primers GFP*AscI*F and GFPpolylinkerR. This PCR fragment was introduced into the *AscI* and *SacI* sites of pFY124 introducing a new *AvrII* site for the following constructions (Vector pQW154).

The *RAX1* open reading frame was amplified by PCR using the primers RAX1*AscI*F and RAX1*SacI*R. The PCR fragment was inserted into the *AscI* and *SacI* sites of pQW154. The *GCAM1* open reading frame was amplified using the primers GCAM1*AscI*F and GCAM1*AvrII*R. The PCR fragment was inserted into the *AscI* and *AvrII* sites of pQW154. The ORF from the second methionine codon of the *GCAM1* coding sequence (GCAM1s; from +85 to the stop codon) was amplified using the primers GCAM1New *AscI*F and GCAM1*AvrII*R. The PCR fragment was inserted into the *AscI* and *AvrII* sites of pQW154.

The *RAX1pro:RAX1*, *RAX1pro:GCAM1*, and *RAX1pro:GCAM1s* constructs were introduced into the *Arabidopsis rax1-3 rax2-1 rax3-1* mutant [24] using the floral dip method, and T_3 homozygous transgenic lines were used for further analysis.

For cultivation under short-day conditions, *Arabidopsis* plants were grown in a controlled environment room under a 8 h/16 h (light/dark) photoperiod, 20°C/18°C (day/night) temperatures, and 50% relative humidity. Flowering was induced after 4 weeks by transferring the plants to a 16 h/8 h (light/dark) photoperiod. Cultivation under long-day conditions was done in a controlled greenhouse with additional artificial light when needed.

Axillary bud formation was analyzed after the onset of flowering using a stereomicroscope as previously described [50]. Buds that had produced one or two leaf primordia as well as elongating lateral shoots were scored as leaf axils that had established axillary meristems.

QUANTIFICATION AND STATISTICAL ANALYSIS

We used Welch's t test or Student's t test to evaluate statistical significance as shown in the legends for [Figures 1, 3, and 5](#). Experimental sample sizes and statistical methods detail are given in the legends for [Figures 1, 3, and 5](#). The raw data of axillary bud formation for [Figure 5H](#) is provided in [Figure S5](#).

DATA AND CODE AVAILABILITY

All reads obtained have been deposited in the DDBJ and are available through the Sequence Read Archive (SRA) under the accession number DRA005912. The authors declare that all data supporting the findings of this study are available within the manuscript and its supplementary files or are from the corresponding author upon request.